Journal of Hydrology 409 (2011) 291–304

Contents lists available at SciVerse ScienceDirect

Journal of Hydrology

journal homepage: www.elsevier.com/locate/jhydrol

An ecohydrological model for studying groundwater–vegetation interactions in wetlands

Ting Fong May Chui [a,*], Swee Yang Low [a,b], Shie-Yui Liong [b]

[a] Department of Civil and Environmental Engineering, National University of Singapore, 1 Engineering Drive 2, E1A 07-03, Singapore 117576, Singapore
[b] Tropical Marine Science Institute, National University of Singapore, 21 Lower Kent Ridge Road, Singapore 119077, Singapore

ARTICLE INFO

Article history:
Received 7 October 2010
Received in revised form 20 July 2011
Accepted 10 August 2011
Available online 22 August 2011
This manuscript was handled by
Philippe Baveye, Editor-in-Chief

Keywords:
Ecohydrology
Groundwater drawdown
Land use change
Numerical modeling
Plant biomass
Wetlands

SUMMARY

Despite their importance to the natural environment, wetlands worldwide face drastic degradation from changes in land use and climatic patterns. To help preservation efforts and guide conservation strategies, a clear understanding of the dynamic relationship between coupled hydrology and vegetation systems in wetlands, and their responses to engineering works and climate change, is needed. An ecohydrological model was developed in this study to address this issue. The model combines a hydrology component based on the Richards' equation for characterizing variably saturated groundwater flow, with a vegetation component described by Lotka–Volterra equations tailored for plant growth. Vegetation is represented by two characteristic wetland herbaceous plant types which differ in their flood and drought resistances. Validation of the model on a study site in the Everglades demonstrated the capability of the model in capturing field-measured water table and transpiration dynamics. The model was next applied on a section of the Nee Soon swamp forest, a tropical wetland in Singapore, for studying the impact of possible drainage works on the groundwater hydrology and native vegetation. Drainage of 10 m downstream of the wetland resulted in a localized zone of influence within half a kilometer from the drainage site with significant adverse impacts on groundwater and biomass levels, indicating a strong need for conservation. Simulated water table–plant biomass relationships demonstrated the capability of the model in capturing the time-lag in biomass response to water table changes. To test the significance of taking plant growth into consideration, the performance of the model was compared to one that substituted the vegetation component with a pre-specified evapotranspiration rate. Unlike its revised counterpart, the original ecohydrological model explicitly accounted for the drainage-induced plant biomass decrease and translated the resulting reduced transpiration toll back to the groundwater hydrology for a more accurate soil water balance. This study represents, to our knowledge, the first development of an ecohydrological model for wetland ecosystems that characterizes the coupled relationship between variably-saturated groundwater flow and plant growth dynamics.

1. Introduction

Wetland ecosystems make up approximately 6% of the Earth's land surface (OECD, 1996), occurring in a wide range of habitats including floodplains, marshes, rivers, estuaries and near-shore coastal zones (Davis, 1994). Wetlands provide various critical ecosystem services such as purifying the air and water, mitigating floods and droughts, and supporting wildlife habitats. Despite their importance, wetlands are under threat from human exploitation and climate changes (Jackson et al., 1991; Davis and Ogden, 1994; van der Valk, 2006). In addition, they are often not managed properly or restored successfully due to inadequate understanding of the systems and their responses to management scenarios.

In wetlands, hydrology plays a key role in vegetation dynamics. The shallow water tables facilitate interactions with vegetation roots, supplying water to plants and, through fluctuations in water table levels, influencing the oxygen and nutrient availability (Muneepeerakul et al., 2008). In turn, vegetation affects soil water balance through growth dynamics, transpiration and interception. This strong coupling between vegetation and water tables leads to important and interesting feedbacks between hydrological and ecosystem processes (Ridolfi et al., 2006; Rodriguez-Iturbe et al., 2007; Laio et al., 2009). Thus, there is strong motivation to understand better these main wetland components, i.e., the hydrologic and vegetation systems, to help guide efforts in their protection and restoration.

Ecohydrological models provide a potentially useful tool in characterizing groundwater–vegetation interactions. Prior studies

* Corresponding author. Address: Department of Civil and Environmental Engineering, Block E1A, #07-03, 1 Engineering Drive 2, National University of Singapore, Singapore 117576, Singapore. Tel.: +65 6516 7104; fax: +65 6779 1635.
E-mail address: ceectfm@nus.edu.sg (T.F.M. Chui).

0022-1694/$ - see front matter © 2011 Elsevier B.V. All rights reserved.
doi:10.1016/j.jhydrol.2011.08.039

have investigated the coupled relationship between vegetation change and groundwater depth in arid regions (Fred, 1981; Huete, 1988; Krysanova et al., 1989; Poiani and Johnson, 1993; Harry and Wassen, 1997; Gullison and Bourque, 2001; Zhao et al., 2005; Tietjen et al., 2010;). However, these models do not account for long-lasting saturated conditions and thus their ecohydrological application has been limited to instances where the significant groundwater depth exerted little or no influence on the soil water balance (Laio et al., 2009). For wetlands, ecohydrological studies have coupled plant growth equations with soil water-balance bucket models (Muneepeerakul et al., 2008; Laio et al., 2009) to study long-term system behaviors under conditions such as climate change, or have applied variably-saturated groundwater models (Freeze, 1971; Boswell and Olyphant, 2007), without explicitly accounting for vegetation dynamics, to provide information on regularly and rarely saturated areas favoring different plant types.

To address the need for elucidating dynamic groundwater–vegetation interactions in wetlands to help guide management and restoration efforts, an ecohydrological model was developed in this study that couples variably-saturated groundwater models with established plant growth equations. To our knowledge, this is the first development of a coupled model for wetlands describing spatially varying groundwater movement and explicitly accounting for interdependent plant growth dynamics. The model facilitates study of the sensitivity of hydrological and vegetation response to land use change and climate change. To demonstrate model capability, the model was applied, using currently available generic wetland soil and plant parameters, to a tropical wetland in Singapore, the Nee Soon swamp forest, in order to elucidate the ecohydrological impact due to hypothetical construction drainage caused by downstream engineering works.

2. Methods

This section first describes the ecohydrological model that involves groundwater modeling (Section 2.1) and vegetation modeling (Section 2.2), as well as the coupling of the groundwater and plant growth components (Section 2.3). It then explains the simulations, carried out to validate the model (Section 2.4), to demonstrate the potential impact of a drawdown (Section 2.5) and the significance of accounting plant growth dynamics (Section 2.6). The conceptual models and assumptions associated with each of the simulations can be found in their corresponding sections.

2.1. Groundwater modeling

The ecohydrological model was developed on COMSOL Multiphysics (COMSOL, Inc., Burlington MA), which provides a unified graphical modeling environment for model formulation, parameter and initial condition specification, mesh generation and post-processing. COMSOL provides robust numerical solvers for user-assembled coupled partial and ordinary differential equations which is crucial to the coupling of variably-saturated groundwater models with established plant growth equations in this study. Different hydrologic boundary conditions (e.g., rainfall infiltration and evapotranspiration) have also been implemented and verified with previous published results (Chui and Freyberg, 2009). Two dimensional variably saturated flow is modeled using the Richards' equation (Eq. (1)), which describes spatially-varying groundwater movement and provides information on soil moisture at different depths:

$$\frac{(C+S_eS)}{\rho_f g}\frac{\partial p}{\partial t}+\nabla\cdot\left[-\frac{K_s}{\rho_f g}k_r\nabla(p+\rho_f gz)\right]=Q_s \tag{1}$$

where ρ_f is the fluid density (kg/m^3), g is the gravitational acceleration (m/s^2), C is the specific capacity (m^{-1}), S_e is the effective saturation (–), S is the specific storage (m^{-1}), p is the fluid pressure (Pa), t is the time (s), K_s is the saturated hydraulic conductivity (m/s), k_r is the relative permeability (–), z is the vertical coordinate (m), and Q_s is the fluid source or sink (s^{-1}).

Approximate numerical solutions of the Richards' equation are implemented using finite elements within the Earth Science module of COMSOL, which streamlines model setup of the Richard's equation for environmental applications. The retention and relative permeability functions are modeled using the well-known van Genuchten forms (van Genuchten, 1980).

2.2. Vegetation modeling

Vegetation modeling simulates plant growth dynamics by computing the biomass of each vegetation type of interests. It accounts for the characteristics of the vegetation type (e.g., growth and decay rate, carrying capacity at different water table depth), as well as its interactions with other vegetation types. Modified Lotka–Volterra equations (Eq. (2)) (Lotka, 1925, 1956; Volterra, 1926, 1931), as previously described in Muneepeerakul et al. (2008), are used to characterize plant growth dynamics for specific demarcated subsections of the study domain:

$$\frac{dB_i}{dt}=B_i\left(r_i\left(1-\frac{\alpha_{ii}B_i+\sum_{j\neq i}\alpha_{ij}B_j}{K_i(y)}\right)-\beta_i\right) \tag{2}$$

where B_i is the biomass of plant type i per unit area (kg/m^2), r_i is the intrinsic growth rate (s^{-1}), α_{ij} is the impact coefficient of plant type j on plant type i (–), $K_i(y)$ is the ecosystem carrying capacity limited by environmental factors (e.g., light, nutrients, water and air in the soil) (kg/m^2), and β_i is the decay rate per unit biomass resulting from senescence and root respiration (day^{-1}). Formulations adopted by Muneepeerakul et al. (2008) for the intrinsic growth rate, biomass decay rate and the water-table dependent carrying capacity have also been applied in this study. The intrinsic growth rate is determined by:

$$r_i=\left(\omega\frac{T_a}{B}\right)_i \tag{3}$$

where ω_i is the intrinsic water use efficiency (kg/m^3), and $(T_a/B)_i$ is the transpiration per unit land area per unit biomass, with T_{ai} being given by:

$$T_{ai}=\frac{\int_{Vi}T_i\,dV_i}{A} \tag{4}$$

where T_i (/s) is the transpiration at a given point in the root zone (Eq. (9)), V_i is the volume of the root zone (m^3) and A is the land area (m^2).

The biomass decay rate is expressed as:

$$\beta_i=R_{ri}(1-f_{Li})+q_i \tag{5}$$

where R_{ri} is the root respiration coefficient (s^{-1}) and q_i is the senescence rate (s^{-1}). The intrinsic water use efficiency ω_i in Eq. (3) is given by the ratio of the maximum assimilation rate, A_{mi} (kg/s m^2) and the potential maximum transpiration rate, T_{pi} (m/s):

$$\omega_i=\left(Y_g\frac{A_m}{T_p}\right)_i \tag{6}$$

where Y_{gi} denotes the growth yield of plant type i defined as the fraction of carbon assimilation that remains after paying above-ground growth respiration costs (–).

The potential maximum transpiration, T_{pi} is given by:

$$T_{pi}=\left(\frac{T_m}{A_L f_L K^*}\right)_i \tag{7}$$

where A_{Li} denotes leaf area per unit aboveground biomass (m^2/kg), f_{Li} is the ratio of aboveground biomass to total biomass (–), K_i^* is the maximum ecosystem carrying capacity of plant species i (kg/m^2), and T_{mi} is the maximum total transpiration per unit land area of plant species i when its biomass is at K_i^*.

The carrying capacity of plant type i is modeled as a function of water table depth, y (m):

$$K_i(y) = K_i^* \left(\frac{y - y_{ci}}{y_{pi} - y_{ci}}\right) e^{\left(\frac{y_{pi}-y}{y_{pi}-y_{ci}}\right)} \quad (8)$$

where y_{ci} is the water table depth below which the carrying capacity of plant type i becomes zero (m). y_{pi} is the water table depth (m) at which the carrying capacity is at the maximum, K_i^* (kg/m^2).

Vegetation is represented by two characteristic wetland herbaceous plant types. The number of plant types has been limited to two in this proof-of-concept study to demonstrate the model's abilities to model the growth for more than one plant type and to differentiate between the behaviors of the different plant types considered. Only herbaceous plant types were considered due to their relatively rapid response to environmental stimuli compared to large woody plant types like trees. The two plant types considered differ in their survival and competition strategies. They have different flood and drought resistances, with the more flood-resistant plant type (Type I) having shallower roots as it tends to keep root biomass away from the saturated zone, and the less flood-resistant plant type (Type II) having deeper roots to uptake groundwater during drought conditions. They thus vary in their behavior in, and response to, changing hydrologic conditions. Plant parameters used in the study represented common and generic wetland herbaceous plant types, and were taken from Muneepeerakul et al. (2008) as shown in Table 1, which were, in turn, derived from Larcher (2001) and Lambers et al. (1998). To prevent the continued extinction of a plant type once its biomass reaches zero, a minimum biomass limit, which is set at 10% of $K_i(y)$, was pre-specified. The specification of this minimum limit provides for resilience to fluctuations in environmental conditions, guarding against irrecoverable plant death and allowing for the future recovery of the plant type, e.g., from seeds or residual biomass. Fig. 1 shows the relationship between ecosystem carrying capacity of Type I (K_1) and Type II (K_2) plants as a function of water table depth. The vertical lines on the graph indicate optimum water table depths corresponding to maximum carrying capacities for both plant types. The optimum depth line demarcates the carrying capacity–water table graph into two zones: an oxygen-limited zone on the left as we approach flooding conditions, and a water-limited zone on the right due to impending drought.

Table 1
Plant parameters used in the simulation for model validation (RG2) and in the Nee Soon study domain simulation (Nee Soon).

Parameter	Plant Type I	Plant Type 2
Impact coefficient of plant type j on plant type i, α_{ij}	$\alpha_{11} = \alpha_{12} = 1$	$\alpha_{22} = \alpha_{21} = 1$
Maximum assimilation rate, A_{mi}	5.8×10^{-7} kg/s m^2	8.1×10^{-7} kg/s m^2
Growth yield of plant type i, Y_{gi}	0.9	0.9
Leaf area per unit aboveground biomass, A_{Li}	5 m^2/kg	5 m^2/kg
Ratio of aboveground biomass to total biomass, f_{Li}	0.2	0.15
Root respiration coefficient, R_{ri}	6.4×10^{-8} s^{-1}	6.4×10^{-8} s^{-1}
Senescence rate, q_i	1.7×10^{-8} s^{-1}	1.7×10^{-8} s^{-1}
Maximum ecosystem carrying capacity, K_i^*	2.5 kg/m^2	2.5 kg/m^2
Critical water table depth, y_{ci}	−1.5 m[a]	−0.9 m
Water table depth at which $K_i = K_i^*$, y_{pi}	0.8 m	1.0 m
T_{mi}	5.8×10^{-8} m/s	5.8×10^{-8} m/s
Mean root length, λ_i	0.45 m	0.55 m
Depth of root zone, D_i	1.2 m	1.5 m

[a] A negative critical water table depth means that there is nonzero biomass even when the soil is completely waterlogged.

Transpiration from vegetation is modeled as sinks within the root zone of the subsurface, which may be above or below the water table. The rate of transpiration at a given point within the root zone, T_i (s^{-1}) is described by the following relationship (Panday and Huyakorn, 2004) that distributes the net capacity for transpiration among several factors:

$$T_i = [f_1(LAI_i)][f_2(\theta)][RDF_i][E_{ref}] \quad (9)$$

where $f_1(LAI_i)$ and $f_2(\theta)$ are functions of leaf area index (–) and water content (–) respectively. They are respectively denoted as:

$$f_1(LAI_i) = \max\{0, \min[1, (C_2 + C_1 LAI_i)]\} \quad (10)$$

where C_1 and C_2 are both fitting parameters (–).

$$f_2(\theta) = \begin{cases} 0 & \text{for } 0 \leqslant \theta \leqslant \theta_{wp} \\ 1 - \left[\frac{\theta_{fc}-\theta}{\theta_{fc}-\theta_{wp}}\right]^{C_3/E_{ref}} & \text{for } \theta_{wp} \leqslant \theta \leqslant \theta_{fc} \\ 1 & \text{for } \theta_{fc} \leqslant \theta \leqslant \theta_0 \\ \left[\frac{\theta_{an}-\theta)}{\theta_{an}-\theta_0}\right]^{C_3/E_{ref}} & \text{for } \theta_0 \leqslant \theta \leqslant \theta_{an} \\ 1 & \text{for } \theta_{an} \leqslant \theta \end{cases} \quad (11)$$

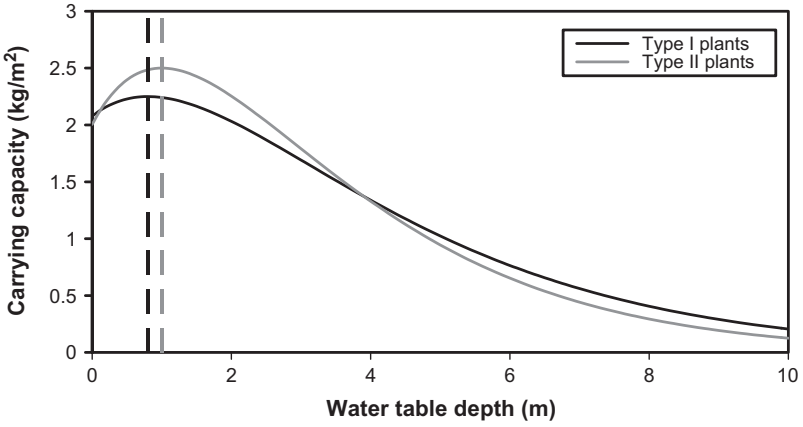

Fig. 1. Ecosystem carrying capacities of the two plant types considered in the study, as a function of water table depth. Vertical lines indicate the optimum water table depths (0.8 m for Type I plants and 1 m for Type II plants) at which the carrying capacities for the respective plant types are the maximum.

where C_3 is a fitting parameter (–), θ_{wp} is the moisture content at wilting point (–), θ_{fc} is the moisture content at field capacity (–), θ_0 is the moisture content at oxic limit (–) and θ_{an} is the moisture content at anoxic limit (–).

The leaf area index (LAI_i) is given by:

$$LAI_i = (A_L f_L B)_i \tag{12}$$

RDF_i is the value of the root distribution function (m^{-1}), and is modeled as an exponential distribution, with the density of the roots being greatest at the land surface:

$$RDF_i = \left(\frac{(1/\lambda)e^{-(1/\lambda)d}}{1 - e^{-(1/\lambda)d}}\right)_i \tag{13}$$

where λ is the mean root depth (m) and d is the depth from the land surface of the point within the root zone under consideration.

The root distribution function is subject to the following constraint which holds for each vertical section of the root zone:

$$\int_{Di} RDF_i \, dD_i = 1 \tag{14}$$

where D_i is the depth of the root zone.

E_{ref} is the reference evapotranspiration rate (m/s), which may be derived from pan measurements or computed from vegetation and climatic factors, e.g., using the Penman–Monteith equation (Monteith, 1981). Soil evaporation is assumed negligible compared to plant transpiration. For this study, field measured reference evapotranspiration rates for the two study domains were used, as shown in Figs. 2 and 5, and as described in more detail in Sections 2.4 and 2.5.

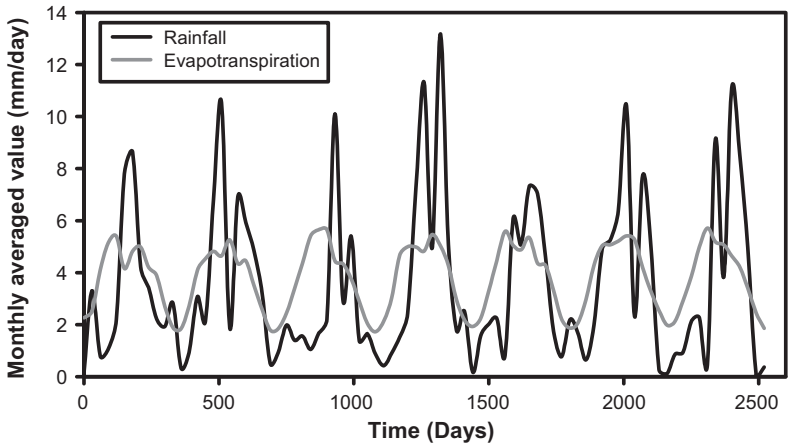

Fig. 2. Field measured rainfall and reference evapotranspiration rates at the RG2 site of the Everglades over a 7-year period, 2002–2008.

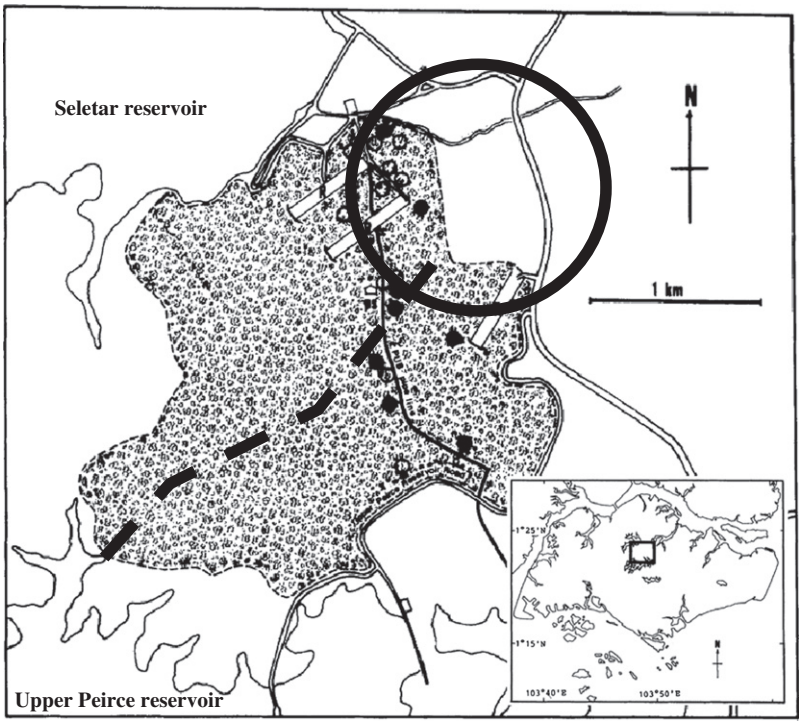

Fig. 3. The Nee Soon swamp forest (Ng and Lim, 1992). The location of possible future construction works is shown circled. The study domain for this paper is indicated by the dotted line. (Inset) Location of the swamp forest in Singapore.

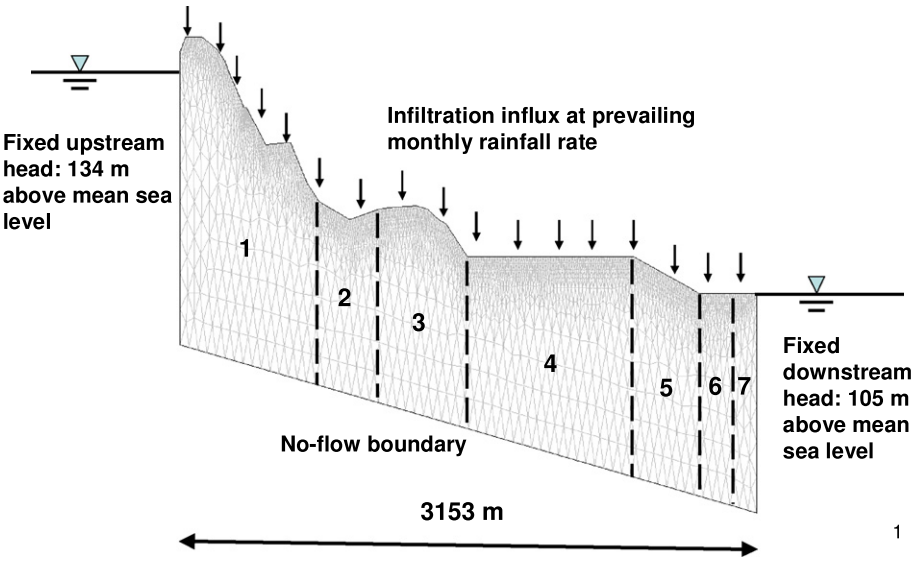

Fig. 4. Model domain in Nee Soon swamp forest for the baseline scenario. The section is about 3 km long and has an upstream head determined by the operating level of the Upper Peirce Reservoir. The water-logged swamp forest fixes the downstream head. For biomass computations, the domain is partitioned into seven subsections as shown, with the approximate width of each section as follows: (1) 760 m; (2) 390 m; (3) 420 m; (4) 910 m; (5) 360 m; (6) 260 m; and (7) 100 m. A finer partitioning was assigned to the more ecologically important downstream wetlands portion (Sections 5–7). The two-dimensional variably-saturated flow modeling on the other hand is across the entire domain.

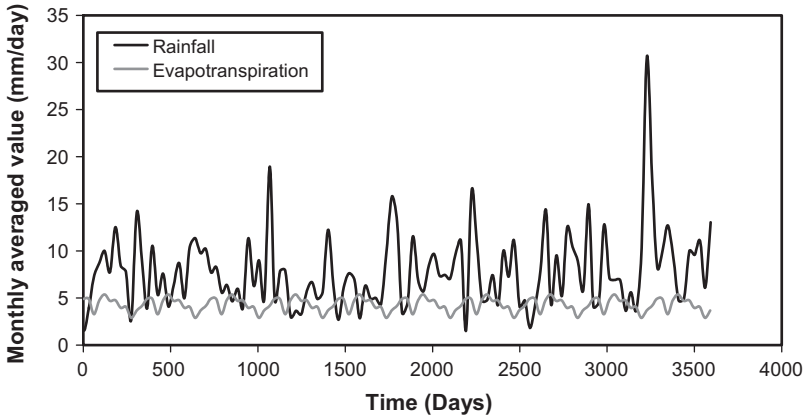

Fig. 5. Field-measured precipitation and evapotranspiration rates used for studying the impact of hypothetical construction drainage on Nee Soon. Precipitation data was collected at the nearby Orchid Mandai station over a 9-year period from 1998 to 2007. Reference pan evapotranspiration rates were taken from 2003 data measured at the Changi climatological station situated in eastern Singapore, and applied annually for the 9-year study period, as indicated in the graph above.

2.3. Coupling groundwater and plant growth components

COMSOL is designed for multiphysics modeling and is capable of solving complete, coupled system of differential equations. Users provide the coupling by specifying the partial differential equations, boundary and condition conditions symbolically. COMSOL then assembles the finite element method description by forming the augmented stiffness matrix (the stiffness matrix, the load vector, and auxiliary equations for Lagrange multipliers representation boundary conditions and auxiliary conditions) (Zimmerman, 2006). Details on the discretization of the equations can be found in COMSOL AB (2008). The time dependent solver algorithm selected for this problem is IDA which was created at the Lawrence Livermore National Laboratory (Hindmarsh et al., 2005). At each time step, a Newton solver is used to solve the nonlinear system of equations. The Newton solver, in turns, uses a direct solver UMFPACK detailed in Davis (2009) for the linearized systems.

In our model, the groundwater component (as described by the Richards' equation, Eq. (1) and the plant growth component (as described by the Lotka–Volterra equation, Eq. (2) are solved simultaneously and are then coupled via transpiration and carrying capacity. Plant biomass, B (Eq. (2)) determines the leaf area index, LAI_i (Eq. (12)), which in turn affects transpiration, T_i (Eq. (9)). This transpiration contributes directly to the sink term, Q_s, in the Richards' equation (Eq. (1)). Conversely, the Richards' equation describes flow in the saturated and unsaturated zones. characterizing hydraulic, pressure and elevation heads and consequently, the water table location, y. The water table influences the carrying capacity for plants, K_i (Eq. (8)), which in turn affects plant biomass, B (Eq. (2)).

2.4. Validation of model

The ecohydrological model was tested using data from the RG2 site of the Everglades as collected by the US Geological Survey, which is available in the public domain (http://sofia.usgs.gov/eden). The terrain is very gently sloping, with a mean slope of ~3–4%. The plants are typical of wet prairie and emergent marsh.

The study domain is assumed to be flat with a rectangular cross-section (2D) which is 5 m deep and 120 m wide. To focus on the groundwater and vegetation dynamics induced by changes in precipitation and evapotranspiration, lateral groundwater fluxes into and out of the domain (expected to be insignificant in comparison) were assumed to be zero. The bottom boundary is a no-flow boundary while the top boundary receives an infiltration influx based on the monthly rainfall rate. We have also precluded modeling for surface water and groundwater–surface water interactions. The average water table for January 2002 was 0.201 m below the land surface, and was taken as the initial value for the start of the simulation. The soil is a fine sand and conditions are assumed to be homogeneous, with soil and transpiration parameters used as shown in Table 2. Each plant type has an initial biomass of 40% of its corresponding maximum carrying capacity. The domain was discretized into ~1200 triangular elements and partitioned into three equal subsections of 40 m each for biomass computations.

The simulation was driven by field-measured precipitation from 2002 to 2008, with transpiration computed from reference evapotranspiration values over the same period (Fig. 2). A seasonal variation with approximately concurrent peaks in rainfall and evapotranspiration could be distinguished every ~350–400 days. Precipitation and evapotranspiration values were averaged over monthly intervals, and the maximum simulation time-step was 10 days. This selected time resolution provided a good balance between computational costs and the ability to capture aggregate responses of the subsurface. Infiltration across the ground surface into the subsurface was at the monthly precipitation rate, and occurred only when the subsurface was unsaturated, i.e., no ponding was considered and any precipitation excess was ignored. The overall simulation lasted a total of over 2500 days (~7 years). Model results were stored at every 30-day interval, and only results for the last 5 years of the simulation were considered for validation to minimize the influence of the choice of initial conditions.

2.5. Impact of drawdown on groundwater–vegetation interactions in Nee Soon

The Nee Soon swamp forest in Singapore was selected as the study area for application of the ecohydrological model to assess the impact of a hypothetical scenario of construction drainage on groundwater hydrology and on the biomass of the plant community. The swamp forest represents the most significant freshwater swamp ecosystem in Singapore. Located in the northern part of the Central Catchments Nature Reserve at an altitude of less than 10 m above present mean sea level (Fig. 3), it is an area of relatively intact, permanently flooded peat swamp forest that covers about 80 ha and is fed by rainfall and drainage from a surface catchment of about 5 km^2. Twenty species of herbaceous species were recorded from three 0.2 ha plots by Turner et al. (1996). Example of species that correspond to Type I plants include Cryptocoryne griffithii and Alocasia denudate, while those that correspond to Type II plants include Aglaonema nitidum and Homalomena.

Anticipated land use changes for possible future development downstream of the swamp raise questions about the impact of engineering works on both the groundwater response and vegetation biomass. To elucidate the effect of this land use change on the hydrology and biota of Nee Soon, a 3 km cross-section of the swamp forest has been demarcated as the study area (Fig. 4). The upstream end of the study area is located at the Upper Peirce Reservoir, with the downstream end located where drainage works for construction would be expected to take place. From known operating levels of the reservoir, a fixed hydraulic head of 134 m (relative to mean sea level) was assigned at the upstream end of the study domain as one of the boundary conditions for the modeling study. For the baseline scenario, a fixed head of 105 m was designated as the boundary condition for the downstream end, where the swamp forest is situated, to signify water tables close to (at) the land surface. The bottom boundary is a no-flow zone while the top boundary receives an infiltration influx based on the monthly rainfall rate. The domain was discretized into 4056 elements and partitioned into seven subsections for biomass computations. The area of significance, the wetland, corresponds to subsections 5–7.

From borehole data, the dominant soil texture is clayey silt, and conditions are assumed to be homogeneous and isotropic with soil and transpiration parameters used shown in Table 2. The generic wetland plant parameters as described earlier were deemed to be applicable to Nee Soon, and suffice in this investigation to demonstrate the capability of the model. However, no field measurements were available to fine tune the values. Precipitation data collected at the nearby Orchid Mandai Station (approximately 2 km north of Nee Soon) over a 9 year period (1998–2007) was used to drive the transient simulations, while 2003 pan evaporation data from the Changi climatological station (approximately 20 km east of Nee Soon, the only station where pan evaporation rates are available in Singapore) was used for the reference evapotranspiration rates (Tan et al., 2007) (Fig. 5).

To obtain an initial condition, a constant rainfall rate of 7.8 mm/day and an evapotranspiration rate of 4.3 mm/day (based on the respective averages of the available field data) was applied to the study domain, as well as initial biomass estimates of 1.2 kg/m^2 for Type I plants and 1.1 kg/m^2 for Type II plants. This yielded a steady state solution for the water table, which was subsequently used as the initial condition for the transient simulation. The subsequent baseline transient simulation lasted a total of 3285 days (9 years) and results for the last 7 years of the simulation were taken for analysis.

To analyze the potential impact of a hydraulic head drawdown due to engineering works, a transient simulation was repeated from the same steady state solution. However, after 1095 days (3 years), the boundary condition at the downstream end was revised to 95 m to represent construction drainage. This 10 m drop in hydraulic head was implemented over a period of 1 week and was maintained at that level until the end of the simulation, which continued for another 6 years after the drainage.

The simulations were set up with the best available information for Nee Soon. It is important to acknowledge that there was no significant site characterization and calibration for the soil and vegetation parameters. Therefore, the simulations serve to demonstrate the capability of the model, and can only model and predict

Table 2
Soil and transpiration parameters used in the simulation for model validation (RG2) and in the Nee Soon study domain simulation (Nee Soon). Soil and transpiration parameters are from Wise et al. (1994) and Panday and Huyakorn (2004) respectively.

Parameter	RG2	Nee Soon
Soil porosity	0.46	0.44
Residual moisture content	0.01	0.275
Hydraulic conductivity	5.9×10^{-5} m/s	7.9×10^{-6} m/s
Specific storage	5×10^{-5} m	1.9×10^{-3} m
van Genuchten parameter, α	2.0 m^{-1}	1.05 m^{-1}
van Genuchten parameter, n	2.8	1.23
Dimensionless transpiration fitting parameter, C_1	0.3	0.3
Dimensionless transpiration fitting parameter, C_2	0.2	0.2
Dimensionless transpiration fitting parameter, C_3	3×10^{-6}	3×10^{-6}
Wilting point moisture content, θ_{wp}	0.09	0.09
Field capacity moisture content, θ_{fc}	0.15	0.14
Oxic limit moisture content, θ_o	0.46	0.44
Anoxic limit moisture content, θ_{an}	0.46	0.44

the hydrologic and vegetation systems in a general and generic manner.

2.6. Significance of accounting for plant growth dynamics

To test the significance of accounting for plant growth dynamics on groundwater hydrology, compared to pre-specifying an evapotranspiration rate based on reference values in many commonly adopted hydrological models (e.g., MODFLOW (USGS), HydroGeoSphere (ScienceSoftware)), the simulation with a hypothetical downstream drawdown was repeated with a revised model. In this model, the Lotka–Volterra plant growth equations have been removed, and constant values were specified for the leaf area index functions $f_1(LAI)$ (Eq. (10)) in the transpiration relation based on average biomass levels in each of the seven subsections at the end of the initial 3-year simulation. The constant index function values thus defined are shown in Tables 2 and 3. The motivation for specifying the evapotranspiration rates through constant *LAI* values, instead of directly assigning fixed rates, was to preserve the option of still being able to apportion the evapotranspiration incrementally with decrease in rooting depth (Eq. (9)).

3. Results

3.1. Model validation

Time-dependent water table levels and evapotranspiration rates from the RG2 domain simulations were compared to monthly-averaged field measurements to assess model performance (Fig. 6). For water tables, the field measured values do not exceed 1.1 m below the land surface during the 5-year validation period. Slight ponding of not more than 6 cm was observed at around the 600–660-day and 1740-day marks, possibly as a result of persistent or high rainfall during the closely-corresponding periods in the field at around the 1260–1320-day and 2400-day marks (Fig. 2) (rainfall data preceded the model comparison period by 2 years). A cyclical pattern could approximately be observed, with five peaks and troughs in water table levels over the study period, corresponding approximately with peak rainfall events in the driving precipitation. This cyclical pattern was captured by the model results. The horizontal sections in the modeled water table graph indicate levels that have reached the surface. Two of these horizontal sections occur concurrently with the ponding periods for the field measurements as described earlier, with the other also occurring during a peak in the field-measured water table level (less than 0.2 m below the surface). The model underestimated the field water table levels at around the 210–360-day and 1620–1680-day marks (by a maximum of ~1 m), while overestimating the field values at around the 1350-day mark (by ~0.4 m). Factors that would cause differences between field data and model results are discussed in Section 4.1. A cyclical pattern was also observed in the reference evapotranspiration rates, which also corresponded closely with peak events in the driving precipitation. The model results closely reflected the field reference values. Additional dips in model results were observed at around the 180 and 1600-day marks.

3.2. Outcome of groundwater drawdown

Following validation, the ecohydrological model was applied to a study domain in the Nee Soon swamp forest in Singapore to assess the impact of a hypothetical construction drainage on the

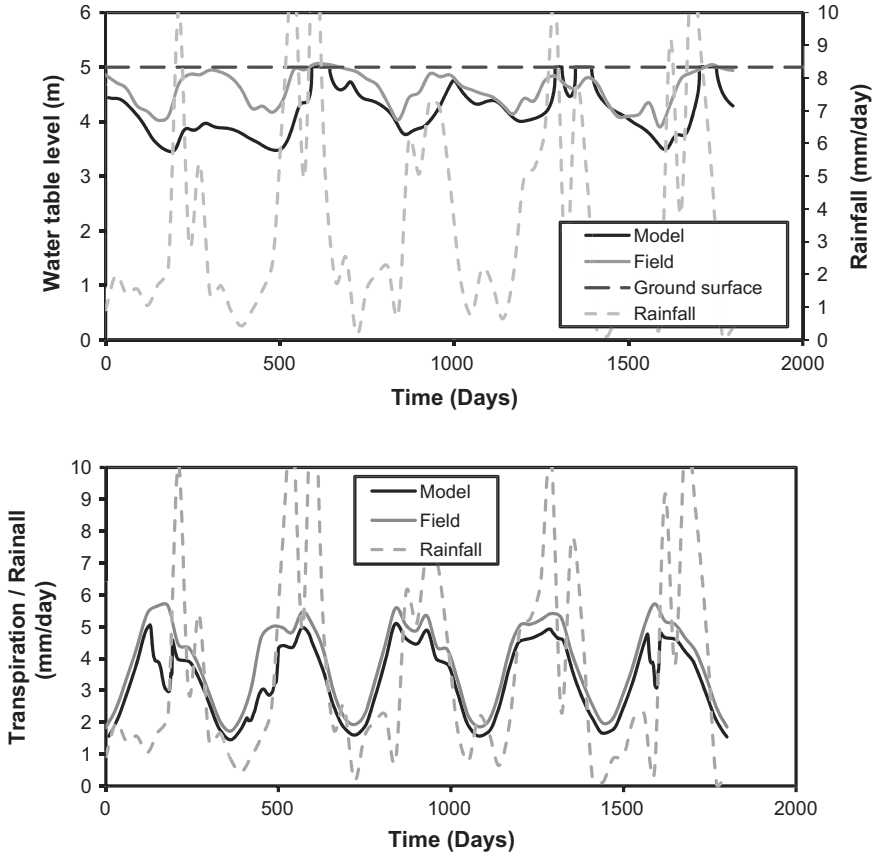

Fig. 6. Comparisons of simulated water table levels (a) and evapotranspiration rates (b) with field-measured values for the RG2 domain of the Everglades. Transient simulations were carried out over a 7-year period (2002–2008) and results from the last 5 years were compared for model validation. The precipitation data has been superposed for reference.

Table 3
Constant leaf area index (*LAI*) values specified for each subsection of the study domain (Fig. 4) in the revised biomass-less model, used for the computation of transpiration.

Subsection	Type I *LAI*	Type II *LAI*
1	0.33	0.56
2	0.58	0.30
3	0.49	0.38
4	0.54	0.34
5	0.52	0.36
6	0.55	0.34
7	0.54	0.35

groundwater hydrology and vegetation. The predicted water table levels at the end of each year for the baseline and drawdown scenarios were compared, from the start of the construction drainage (Fig. 7). The results indicate that the greatest impact on water table levels due to construction drainage was felt in the last two subsections (within the wetlands region of the domain), or up to about 320 m from the location of the drawdown. On average, water table levels decreased by about 6.2 m in the last subsection, and by about 1.1 m in the penultimate subsection.

The last subsection demonstrated the greatest drawdown in water table levels as a result of the drainage, and is expected to display the greatest impact on vegetation compared to the baseline. Fig. 8 focuses on this last subsection in showing the temporal variation in average water table levels and average plant type biomass levels between the baseline and drawdown scenarios. The graph indicates that the water table levels started decreasing almost immediately (~1 day) after the start of construction drainage from levels otherwise observed in the baseline scenario (Fig. 8a). The water table levels took about 85 days to reach a state of dynamic equilibrium from the start of groundwater drawdown, which was completed in a week. Water table levels in the subsection after drawdown were observed to be subjected to greater fluctuations than before the drainage (standard deviation of 0.89 m after drawdown compared to 0.0053 m before drawdown), as the drainage resulted in a greater unsaturated subsurface permitting for more infiltration of rainfall and subsequent response of the water table.

For vegetation, the time taken to respond to the drawdown is longer: about 8–10 days before a response was initiated for both plant types. The biomass levels also took longer to reach a state of dynamic equilibrium: ~100 days. Both plant types have been significantly adversely affected as a result of the drainage, with Type I losing over 53% and Type II losing over 92% of their pre-drainage biomass values (Fig. 8b and c). For Type II plants, the biomass levels have dropped to that for the minimum specified limit. The biomass levels of both plant types were also observed to fluctuate to a greater extent post-groundwater drawdown (Type I: coefficient of variation (COV) of 0.19 after drawdown versus 0.017 before drawdown; Type II: COV of 0.42 after drawdown compared to 0.023 prior), driven by the greater water table changes after drawdown as noted earlier.

On average, total biomass levels (Type I plus Type II) have decreased by about two-thirds (1.77–0.60 kg/m^2) as a result of the drawdown, compared to the baseline scenario (Fig. 8d).

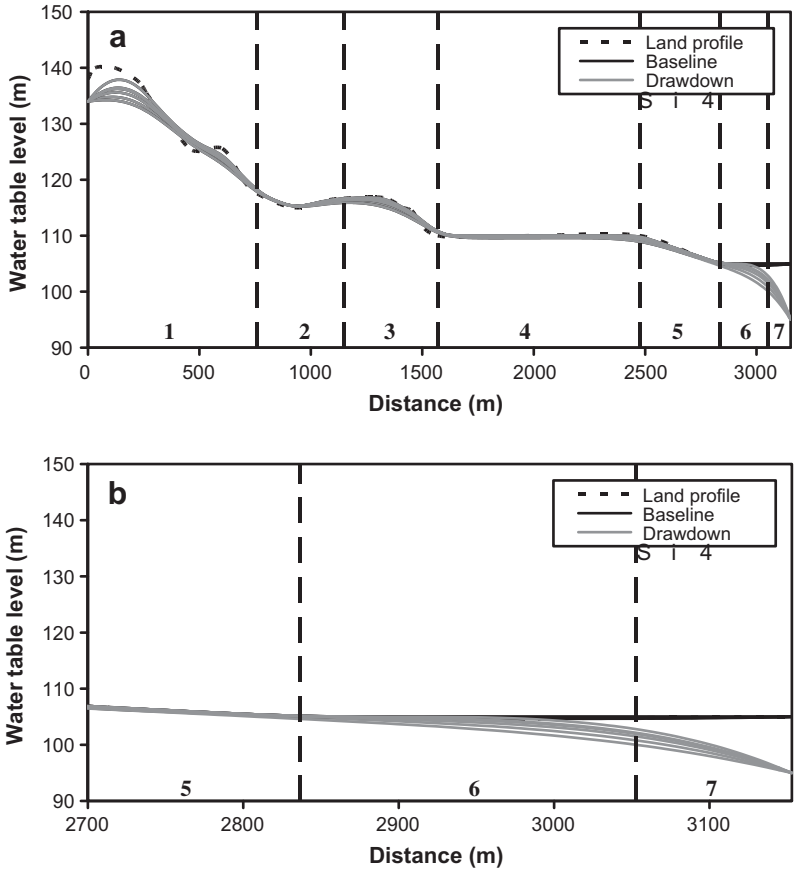

Fig. 7. Water table levels at the end of each year for the baseline (▬) and drawdown (▬) scenarios, in the 6-year simulation since construction drainage began, for the study domain in the Nee Soon swamp forest. The land profile, indicated by the dotted line, is masked in subsections 6–7 by water table levels at the land surface in the baseline scenario. Coincident water table levels in the baseline and drawdown scenarios were observed over subsections 1–5. (a) Results for the entire domain. (b) Results for the last two subsections.

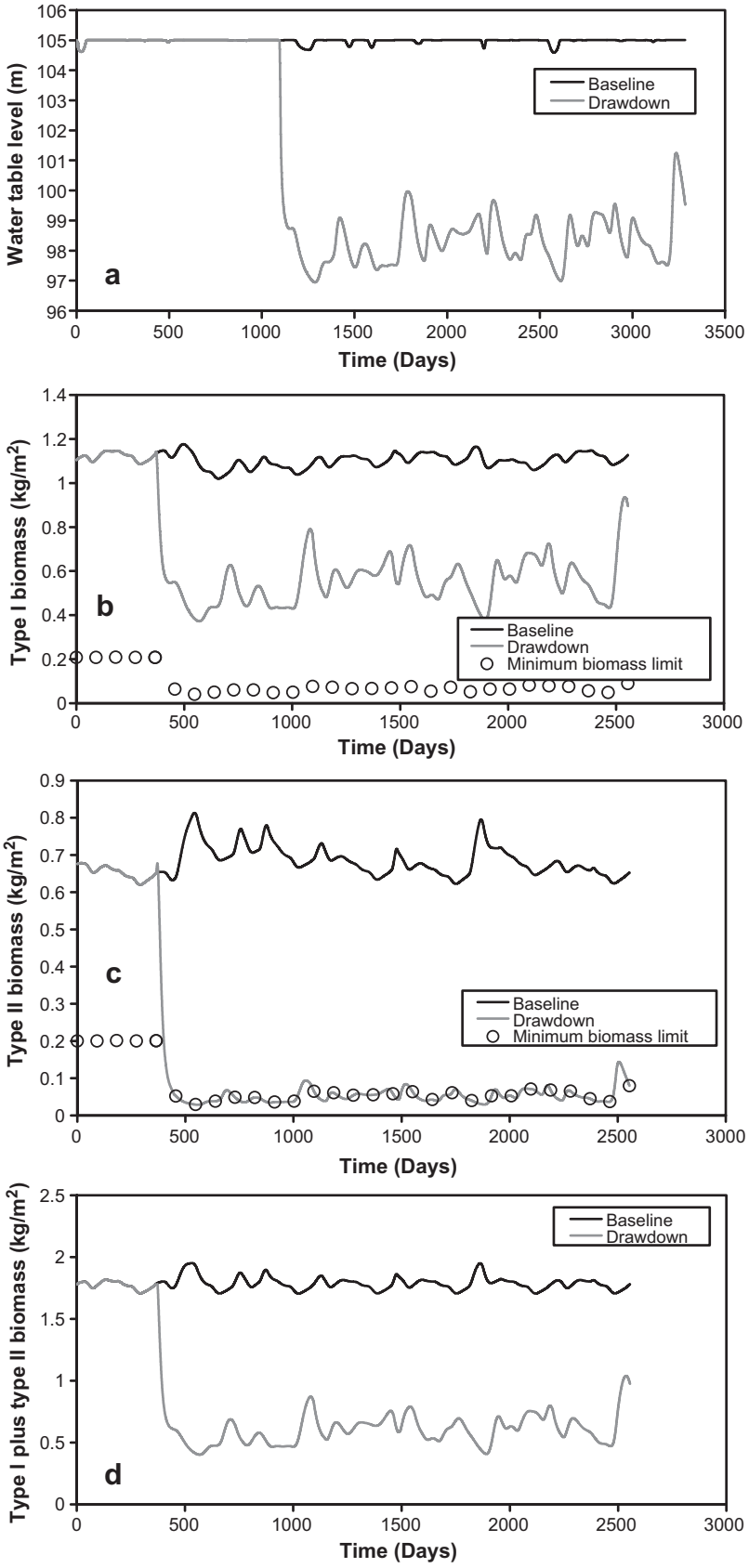

Fig. 8. Temporal variation in average water table levels (a), plant biomass levels (b and c) and total biomass levels (d) in the baseline (▬) and drawdown (▬) scenarios for the last subsection. Minimum biomass limits (○) for the respective plant types are also indicated (b and c). Simulations were run over a 9-year period, with the results for the last 7 years considered for analysis.

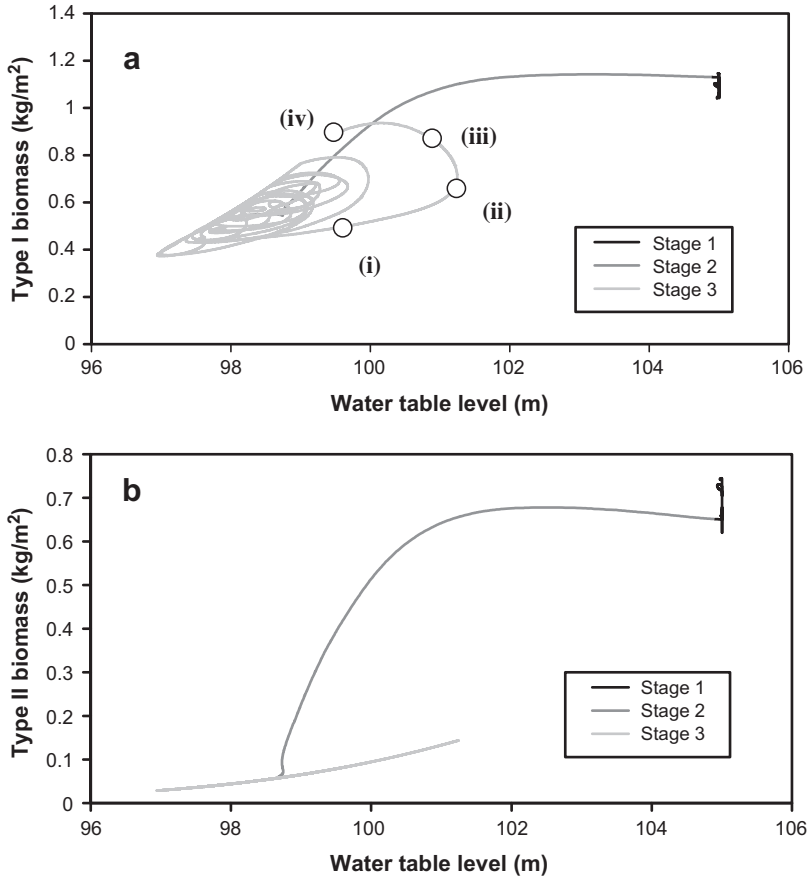

Fig. 9. Variation in Type I (a) and Type II (b) biomass levels against corresponding water table levels for the last subsection. The stages refer to the following: (1) before both water table and biomass levels responded to drawdown; (2) as water table and/or biomass levels were responding to drawdown; (3) both water table and biomass levels have completed responding to drawdown. The four Points (i)–(iv) represent chronologically successive time-points in the water table–biomass relationship that forms part of the characteristic "spiral" pattern displayed by the graph.

3.3. Correlating water table and plant biomass levels

Average biomass values in the last subsection were plotted against corresponding average water table levels with the progression of simulation (Fig. 9), as delineated into three distinct stages: (1) before water table and biomass levels responded to drawdown; (2) as water table and/or biomass levels were responding to drawdown; and (3) after water table and biomass levels have completed responding to drawdown.

The graphs indicate a general trend, for both plant types, in which biomass levels decreased with decreasing water table levels. Before drawdown effects were felt (Stage 1), Type I and Type II biomass levels ranged from ~1.06 to 1.13 kg/m^2 and 0.63 to 0.73 kg/m^2 respectively for a water table elevation of ~105 m. During the start of Stage 2, only water tables were responding to the drawdown, and biomass levels remained at 1.11–1.13 kg/m^2 (Type I) and 0.64–0.65 kg/m^2 (Type II) while water table levels decreased from 105 m to ~101 m. When biomasses started responding, 7–9 days later, along with water tables, the biomass levels decreased from 1.11 to 0.63 kg/m^2 (Type I) and 0.55 to 0.05 kg/m^2 (Type II) for a decrease in water table levels from 101 m to 98.5 m. Towards the end of Stage 2 (for ~22–24 days), only biomasses were responding to the drawdown (due to the inherently slower response time), during which levels ranged from 0.55 to 0.51 kg/m^2 (Type I) and 0.05 to 0.04 kg/m^2 (Type II) for water table levels at ~98.5 m. For the final stage, when both water tables and biomasses have completed their responses to the drawdown, biomass levels ranged from 0.38 to 0.93 kg/m^2 (Type I) and 0.03 to 0.14 kg/m^2 (Type II), for water table levels varying from ~97 m to 101 m. A distinctly irregular, "spiral" pattern was observed for the Type I biomass graph at this last stage (Fig. 9a).

3.4. Comparisons between accounting for biomass and using pre-specified evapotranspiration rate

The ecohydrological model was subsequently applied to compare simulation results for water table levels when modeling for plant type biomass has been included, and when the biomass component has been substituted with pre-specified evapotranspiration rates as defined in Section 2.6.

Fig. 10 shows the water table variations in the last subsection for the 6-year simulation period (after the onset of construction drainage) when biomass computations have been taken into account ("Biomass"), and when they have been precluded ("Specified evapotranspiration"). Water table levels obtained in the simulation where biomass fluctuations were accounted for (mean: 98.37 ± 0.13 m standard error) were found to be significantly higher than in the simulation where the vegetation have been substituted by a pre-specified rate (mean: 98.16 ± 0.14 m) ($p < 0.05$, paired t test). The time taken for the water tables to respond to the drawdown was approximately the same for both the biomass model and the model with the pre-specified evapotranspiration rate (~80 days). Consistent trends were observed for the evapotranspiration results (used as a surrogate for biomass here), in which evapotranspiration rates after drawdown were found to be significantly lower for the model accounting for

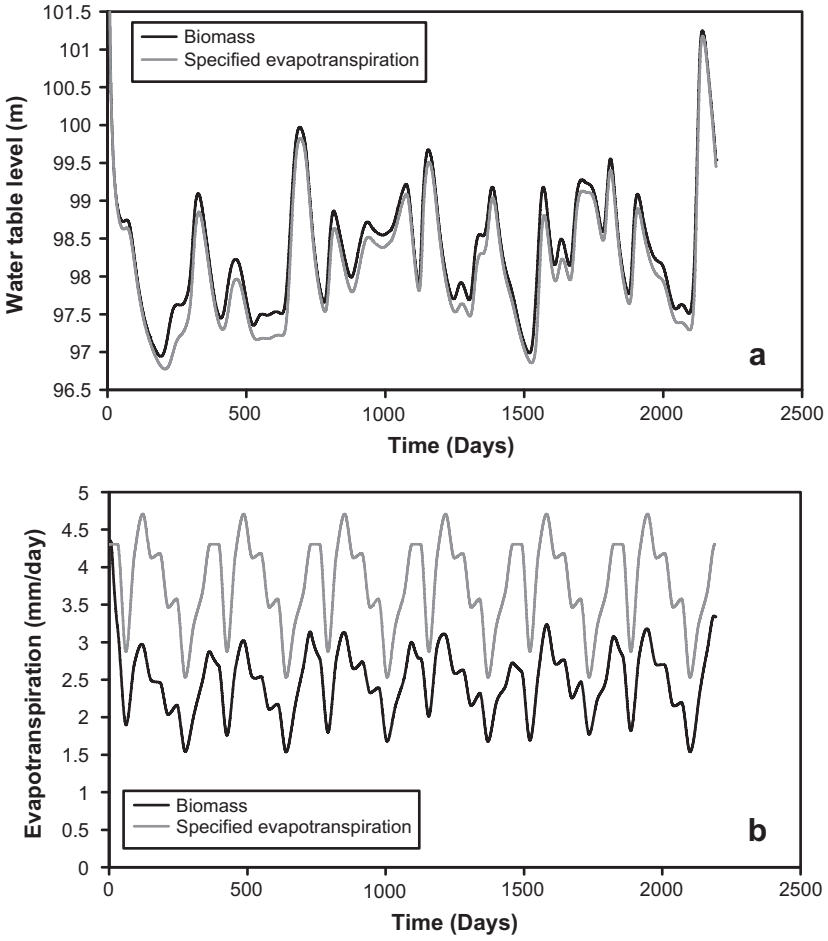

Fig. 10. Average water table levels (a) and evapotranspiration rates (b) in the last subsection of the study domain, as characterized by the model with the biomass component (▬) and the model with pre-specified evapotranspiration rates based on constant leaf area index values (▬).

biomass (mean: 2.51 ± 0.11 mm/day) compared to the pre-specified rate model (mean: 3.80 ± 0.15 mm/day) ($p < 0.05$, paired t test). General simulated trends in water table levels and evapotranspiration rates were observed to be largely similar between the two models.

4. Discussion

4.1. Model capability in simulating field-measured dynamics

The validation process indicated that the model is capable of capturing dynamics of water table and evapotranspiration (used as a biomass surrogate, since no field data is available for comparison) (Fig. 6). The cyclical variations in the water table levels and evapotranspiration rates as driven by field-measured precipitation were simulated in the model results. Several instances of underestimates and overestimates of the field measurements were observed, and could have been attributed to coinciding periods of, respectively, low rainfall (0.50–2.20 mm/day from day 690 to 900 and 0.10–2.26 mm/day from day 2130 to 2310) and high rainfall (10.45 mm/day at day 2010) (Fig. 2), which were not reflected in the corresponding field-measured water table levels. In addition, the assumption of an isolated water table could have overlooked the presence of groundwater fluxes into and out of the RG2 domain in the field. The assumption of a flat domain in our model, which also would affect computations of water table levels relative to the surface, might also be a factor.

4.2. Impact assessment of drainage due to construction works

The validated model was next applied in a case study to assess the impact of a hypothetical drainage due to construction works on the hydrology and vegetation of the Nee Soon swamp forest in Singapore. The novel coupling of a spatially varying groundwater component with plant growth relations means that regional impacts on water tables, and consequently plant biomass, can be modeled precisely, which would otherwise not have been possible had spatially-averaged models such as the soil water balance "bucket" model been used. The results suggest that the impact due to localized drainage is likely to be spatially limited, confined to within 400 m from the location of the construction works. This might be due to the assumption of an isotropic medium for our analysis, which could have underestimated the hydraulic conductivity in the lateral direction and thus the possibility of drainage effects propagating further upstream. Nevertheless, the impact within the zone of influence on groundwater levels (decrease of more than 6 m) and biomass levels of both plant types (losing about two-thirds of combined biomass) was shown to be noticeably severe. The impact also appeared to be felt relatively rapidly, on a timescale of days, with water tables taking ~1 day to respond and the vegetation understandably slightly longer at ~8–10 days. The time taken to reach dynamic equilibrium from the start of groundwater drawdown was about 85 days for water tables and 100 days for biomasses. The relatively rapid decline of the two plant types (with Type I losing half of its biomass and Type II more than 90%) to the construction drainage could have been due to the

severity of the drawdown, and exacerbated by the fact that herbaceous plants were considered. Prior studies also noted significant changes in growth of herbaceous plants on a timescale of 100 days or less as a response to pollution (Honour et al., 2009), CO_2 levels (Wang et al., 2004), and temperature (Furness and Grime, 1982).

It is worth noting that Type II plants, which have deeper roots and therefore might be expected to better adapt to the drawdown, were shown in the simulations to be even more adversely impacted by the drawdown than Type I plants, having been reduced to the minimum biomass level (Fig. 8c). However, this could be attributed to the severe drawdown in the last subsection of more than 6 m, which has resulted in a corresponding sharp decrease in the carrying capacities for both plant types, and in particular, a greater carrying capacity reduction for Type II plants (Fig. 1). The magnitude of drawdown indicates a water-limited ecosystem and drought stresses as the primary factors behind the decline in carrying capacities.

Before drawdown, the average water table depth in the last subsection was approximately 0 m (i.e., the water table was at the land surface), yielding carrying capacities of $\sim$2 kg/m^2 for each plant type. After drawdown, the average depth was more than 6 m below the surface, causing carrying capacities of Type I plants to fall to $\sim$0.6 kg/m^2, and for Type II plants to fall to $\sim$0.5 kg/m^2. This greater rate of decrease in the ecosystem carrying capacity for Type II plants once water table depths exceed $\sim$4 m (Fig. 1), plus its greater biomass decay rate (0.006175 day^{-1} compared to 0.0059 day^{-1} for Type I) could have contributed to the precipitous decrease in Type II biomass levels down to the pre-specified minimum limit.

4.3. Implications for water table–plant biomass relationships

Water table depth is a crucial factor in determining the zonation of vegetation in wetland areas (Dwire et al., 2006). Prior studies have related groundwater levels measured in wells situated at various locations in riparian regions with observed prevailing plant types in order to establish empirical water table depth–vegetation distribution relationships (Ridolfi et al., 2006; Loheide and Gorelick, 2007).

The results (Fig. 9) indicate that, in the state of dynamic equilibrium prior to drainage (Stage 1), biomass levels for both plant types were subjected to little variation (a change of 0.1 kg/m^2 or less) due to relatively constant water table levels close to or at the surface, making field-measured correlations between plant type percentages and water table levels relatively accurate. However, during the subsequent period when water tables and biomasses were affected by the drawdown (Stage 2), the difference in response times between water tables and biomasses means that water table levels could decrease by up to 4 m without a corresponding change in biomass levels, indicating that measurements taken in the field linking the two quantities might not yield accurate relationships.

In the final stage (Stage 3) of dynamic equilibrium, post-drawdown effects, noticeably greater fluctuations and irregular trends could be observed in the water table–biomass relationship for Type I plants (Fig. 9a). Despite the irregular trends, a general tendency of biomass levels for Type I plants to decrease with decreasing water table levels could still be observed, consistent with expectations for the flood-resistant species. The time-lag required for biomass levels to respond to water table fluctuations, thus causing the two quantities to be out of sync with each other, is the postulated reason for the "spiral-shaped" irregular trend observed. Hence, following the chronologically successive Points (i), (ii), (iii) and (iv) in Fig. 9a, the increase in water table levels from Point (i) to Point (ii) resulted in an increasing rate of change in the biomass levels, as the vegetation became increasingly responsive to the water table changes. As water table levels dropped from Point (ii) to Point (iii), the delay in biomass response meant that biomass levels did not correspondingly decrease and continued to increase from the earlier water table rise. Finally, from Point (iii) to Point (iv), biomass levels finally responded to the continuing water table drop, and decreased accordingly, thus yielding the "spiral" pattern observed. With the continuous rise and fall in water table and biomass levels with time, the pattern was repeated, with the size of each "spiral" determined by the magnitude of increase and decrease in levels.

The overall "spiral" pattern resulting from the time-lag effect formed an envelope in which a range of water table levels can be expected for a certain biomass value, and vice versa. The range is noticeably narrower towards lower water table levels ($\sim$97 m) than higher water table levels ($\sim$101 m), and could be attributed to lower carrying capacities at lower water table levels presenting higher drought stresses and inhibiting biomass changes, and vice versa for higher water table levels. Comparatively, for Type II plants, the decrease of biomass levels to the minimum limit as a result of the drainage has meant that variations in biomass levels ($\sim$within a range of 0.1 kg/m^2) and irregular trends due to any time-lag effects, are relatively more limited (Fig. 9b). As with Type I plants, a general trend for the decrease in biomass levels with water table elevations could be perceived as the expected response to increasing drought stresses.

In addition, the ranges of water table and biomass levels (for both plant types) were observed to overlap between Stages 1 and 2, and between Stages 2 and 3. Therefore, depending on whether the system is currently responding to drawdown or is in the state of dynamic equilibrium, very different results can be obtained for field measured water table–plant biomass correlations. For instance, a water table depth of 100 m would give a Type II biomass level of 0.51 kg/m^2 during drawdown, but only 0.095 kg/m^2 after drawdown. Conversely, a Type II biomass level of 0.63 kg/m^2 could be correlated with a water table depth of 105 m before drawdown, and 100.8 m after drawdown.

This overlap, together with the time-lag factor as described earlier, could render uncertainty to water table–plant biomass relationships measured in the field. Without any knowledge of the current state of the system during the period when the survey was conducted, we lack a frame of reference upon which the measurements can be compared. The results for this analysis thus provide motivation for the application of ecohydrological models for studying time-dependent correlations between water table and biomass levels. Such simulation studies could then be validated by, or be used to inform baseline conditions for supporting, field surveys for actual ground conditions.

4.4. Importance of characterizing plant biomass on groundwater hydrology

Prior studies have demonstrated that biota (e.g., plants, fungi, pollen) display significant physiological changes in response to environmental conditions (Abbas et al., 1995; Klironomos et al., 1997; Ahlholm et al., 1998; Gange et al., 2007), and that a direct measurement of these physiological changes, rather than indirect or surrogate measurements, is necessary to clarify the relationship between the environment and biota response (Low et al., 2009).

By explicitly modeling for time-dependent biomass growth and decay with changing hydrologic and weather conditions, the ecohydrological model directly accounted for this physiological vegetation response to environmental conditions, and subsequently characterized its feedback to the groundwater hydrology (Fig. 10). The study results clearly indicate that predicted water table levels between the two models were significantly different during drawdown and in the subsequent dynamic equilibrium

stage when water table levels were below the land surface. In previous discussions, biomass levels for both plant types were observed to decrease as a result of the drawdown, and this drop in total biomass levels in the system would be expected to affect transpiration and therefore impact the groundwater hydrology. The results show that the biomass-inclusive model characterized this decreased transpiration toll and the consequently higher water table levels, demonstrating the importance and need for directly modeling time-dependent biomass changes instead of indirectly accounting for plant biomass through the pre-specification of an evapotranspiration rate.

5. Summary and conclusions

An ecohydrological model was developed in this study characterizing the interactions between interdependent groundwater hydrology and vegetation systems in wetland ecosystems. To our knowledge, the model is the first of its kind, and hence unique, in coupling a fully-distributed, variably saturated groundwater component with a plant growth component describing biomass levels in designated sub-domains for wetland environments. Validation of the model using data from the Everglades indicated that the model was able to accurately simulate fluctuations in water table levels and transpiration rates measured in the field.

Application of the model for studying the effects of a hypothetical construction drainage on a study domain of the Nee Soon swamp forest in Singapore pointed to localized but potentially severe impacts on groundwater hydrology and plant biomass, with possible implications for water management and biodiversity. In particular, the near decimation of Type II (less flood-resistant) plant type, being reduced to the minimum biomass limit, in response to the 10 m hydraulic-head drawdown caused by the drainage, was a significant area for concern. This suggests that strong conservation measures which could, for instance, help raise the minimum biomass limit in order for the plant type to remain competitive in the ecosystem, might be necessary.

Correlations between modeled water table and biomass levels demonstrated a time-lag in the response of biomasses to water table changes, and overlaps in the range of values of water table and biomass levels between stages of dynamic equilibrium and transitional response to drawdown. These factors would impart uncertainty to any field-surveyed observations linking water table and biomass levels. Hence, there is motivation for the use of ecohydrological modeling which could clarify this temporal aspect and comprehensively characterize water table–biomass relationships for different ecosystem states. Further support for the relevance of the model was provided when comparing simulation results with a revised model where the plant growth component has been replaced with a pre-specified evapotranspiration rate. Unlike this revised model, the original model, by being able to explicitly account for temporal biomass variations, was shown to be capable of translating changes in biomass levels (e.g., in response to drainage works) into the feedback of transpiration toll on groundwater hydrology.

Further research should consider the importance of surface hydrology (e.g., streamflow) and groundwater–surface water interactions, as well as the possible implications of altered precipitation patterns due to climate change, on ecosystem hydrology and vegetation.

Acknowledgements

This work was supported by funding from the Ministry of Education, Singapore and the Tropical Marine Science Institute, National University of Singapore. The authors would like to thank the anonymous reviewers for their insightful comments and helpful suggestions.

References

Abbas, H.L., Egley, G.H., Paul, R.N., 1995. Effect of conidia production temperature on germination and infectivity of *Alternaria helianthi*. Ecol. Epidemiol. 85, 677–682.
Ahlholm, J., Helander, M.L., Savolainen, J., 1998. Genetic and environmental factors affecting the allergenicity of birch (*Betula pubescens* ssp. *czerepanovii* [Orl.] Hämet-Ahti) pollen. Clin. Exp. Allergy 28, 1384–1385.
Boswell, J.S., Olyphant, G.A., 2007. Modeling the hydrologic response of groundwater dominated wetlands to transient boundary conditions: implications for wetlands restoration. J. Hydrol. 332, 467–476.
Chui, T.F.M., Freyberg, D.L., 2009. Implementing hydrologic boundary conditions in a multiphysics model. J. Hydrol. Eng. 14 (12), 1374–1377.
COMSOL AB, 2008. COMSOL Multiphysics Reference Guide (Version 3.5a). Stockholm, Sweden.
Davis, T., 1994. The Ramsar Convention Manual: A Guide to the Convention on Wetlands of International Importance Especially as Waterfowl Habitat. Ramsar Convention Bureau, Gland.
Davis, T., 2009. UMFPACK: Unsymmetric Multifrontal Sparse LU Factorization Package. <http://www.cise.ufl.edu/research/sparse/umfpack/> (07.07.11).
Davis, S., Ogden, J., 1994. Everglades 1994: The Ecosystem and Its Restoration. St. Lucie Press, Boca Raton, FL.
Dwire, K.A., Kauffman, J.B., Boone, J., Baham, J.E., 2006. Plant species distribution in relation to water-table depth and soil redox potential in montane riparian meadows. Wetlands 26 (1), 131–146.
Fred, J., 1981. Models of water transport in the soil–plant system: a review. Water Resour. Res. 17 (5), 1245–1260.
Freeze, R.A., 1971. Three-dimensional, transient, saturated–unsaturated flow in a groundwater basin. Water Resour. Res. 7, 347–366.
Furness, S.B., Grime, J.P., 1982. Growth rate and temperature responses in Bryophytes. J. Ecol. 70, 513–523.
Gange, A.C., Gange, E.G., Sparks, T.H., Boddy, L., 2007. Rapid and recent changes in fungal fruiting patterns. Science 316, 71.
Gullison, J.J., Bourque, C.P.-A., 2001. Spatial prediction of tree and shrub succession in a small watershed in Northern Cape Breton Island, Nova Scotia. Can. Ecol. Model. 137, 181–189.
Harry, O.V., Wassen, M.J., 1997. A comparison of six models predicting vegetation response to hydrological habitat change. Ecol. Model. 101, 347–361.
Hindmarsh, A.C., Brown, P.N., Grant, K.E., Lee, S.L., Serban, R., Shumaker, D.E., Woodward, C.S., 2005. SUNDIALS: suite of nonlinear and differential/algebraic equation solvers. ACM Trans. Math. Softw. 31, 363–396.
Honour, S.L., Bell, N.B., Ashenden, T.W., Cape, J.N., Power, S.A., 2009. Responses of herbaceous plants to urban air pollution: effects on growth, phenology and leaf surface characteristics. Environ. Pollut. 157, 1279–1286.
Huete, A.R., 1988. A soil-adjusted vegetation index. Remote Sens. Environ. 25, 295–309.
Jackson, M., Davies, D., Lambers, H., 1991. Plant Life under Oxygen Deprivation: Ecology, Physiology and Biochemistry. SPB Academic, Amsterdam.
Klironomos, J.N. et al., 1997. Increased levels of airborne fungal spores in response to *Populus tremuloides* grown under elevated atmospheric CO_2. Can. J. Bot. 75, 1670–1673.
Krysanova, V., Meiner, A., Roosaare, J., Vasilyev, A., 1989. Simulation modelling of the coastal waters pollution from agricultural watershed. Ecol. Model. 49, 7–29.
Laio, F., Tamea, S., Ridolfi, L., D'Odorico, P., Rodriguez-Iturbe, I., 2009. Ecohydrology of groundwater-dependent ecosystems: 1. Stochastic water table dynamics. Water Resour. Res. 45, W05419.
Lambers, H., Chapin III, F., Pons, T., 1998. Plant Physiological Ecology. Springer, New York.
Larcher, W., 2001. Physiological Plant Ecology: Ecophysiology and Stress Physiology of Functional Groups. Springer, New York.
Loheide, S.P., Gorelick, S.M., 2007. Riparian hydroecology: a coupled model of the observed interactions between groundwater flow and meadow vegetation patterning. Water Resour. Res. 43, W07414.
Lotka, A., 1925. Elements of Physical Biology. Williams and Wilkins, Baltimore, MD.
Lotka, A., 1956. Elements of Mathematical Biology. Dover, New York.
Low, S.Y., Hill, J.E., Peccia, J., 2009. A DNA Aptamer recognizes the Asp f 1 allergen of *Aspergillus fumigatus*. Biochem. Biophys. Res. Commun. 386, 544–548.
Monteith, J.L., 1981. Evaporation and surface temperature. Quart. J. Roy. Meteorol. Soc. 107, 1–27.
Muneepeerakul, C.P., Miralles-Wilhelm, F., Tamea, S., Rinaldo, A., Rodriguez-Iturbe, I., 2008. Coupled hydrologic and vegetation dynamics in wetland ecosystems. Water Resour. Res. 44, W07421.
Ng, P.K.L., Lim, K.K.P., 1992. The conservation status of the Nee Soon freshwater swamp forest of Singapore. Aquat. Conserv. – Mar. Freshwater Ecosyst. 2 (3), 255–266.
Organisation for Economic Co-operation and Development, 1996. Guidelines for Aid Agencies for Improved Conservation and Sustainable Use of Tropical and Subtropical Wetlands. OECD, Paris.
Panday, S., Huyakorn, P.S., 2004. A fully coupled physically-based spatially-distributed model for evaluating surface/subsurface flow. Adv. Water Resour. 27, 361–382.

Poiani, K.A., Johnson, W.C., 1993. A spatial simulation model of hydrology and vegetation dynamics in semi-permanent prairie wetlands. Ecol. Appl. 3 (2), 279–293.

Ridolfi, L., D' Odorico, P., Laio, F., 2006. Effect of vegetation–water table feedbacks on the stability and resilience of riparian plant ecosystems. Water Resour. Res. 42, W01201.

Rodriguez-Iturbe, I., D' Odorico, P., Laio, F., Ridolfi, L., Tamea, S., 2007. Challenges in humidland ecohydrology: interactions of water table and unsaturated zone with climate, soil and vegetation. Water Resour. Res. 43, W09301.

Tan, S.B.K., Shuy, E.B., Chua, L.H.C., 2007. Modelling hourly and daily open-water evaporation rates in areas with an equatorial climate. Hydrol. Process. 21, 486–499.

Tietjen, B., Jeltsch, F., Zehe, E., Classen, N., Groengroeft, A., Schiffers, K., Oldeland, J., 2010. Effects of climate change on the coupled dynamics of water and vegetation in drylands. Ecohydrology 3 (2), 226–237.

Turner, L.M., Boo, C.M., Wong, Y.K., Chew, P.T., Ibrahim, A., 1996. Freshwater swamp forest in Singapore, with particular reference to that found around the Nee Soon Firing Ranges. Gardens' Bull. Singapore 48, 129–157.

van der Valk, A.G., 2006. The Biology of Freshwater Wetlands. Oxford Univ. Press, New York.

van Genuchten, M.T., 1980. A closed-form equation for predicting the hydraulic conductivity of unsaturated soils. Soil Sci. Soc. Am. J. 44 (5), 892–898.

Volterra, V., 1926. Variazone e fluttuazini del numero d'individui in specie animali conviventi. Mem. Acad. Lincei 6, 31–113.

Volterra, V., 1931. Lecons sur la Theorie Mathematique de la Lutte Pour la Vie. Gauthiers-Villars, Paris.

Wang, X., Anderson, O.R., Griffin, K.L., 2004. Chloroplast numbers, mitochondrion numbers and carbon assimilation physiology of *Nicotiana sylvestris* as affected by CO_2 concentration. Environ. Exp. Bot. 51, 21–31.

Wise, W.R., Clement, T.P., Molz, F.J., 1994. Variably saturated modeling of transient drainage: sensitivity to soil properties. J. Hydrol. 161 (1–4), 91–108.

Zhao, C., Wang, Y., Chen, X., Li, B., 2005. Simulation of the effects of groundwater level on vegetation by combining FEFLOW software. Ecol. Modell. 187, 341–351.

Zimmerman, W.B.J., 2006. Multiphysics Modeling with Finite Element Methods. World Scientific, Singapore.